Mechanisms for Coherent Scattering of Electromagnetic Waves from Relativistic Electron Beams

V. L. GRANATSTEIN AND P. SPRANGLE

Abstract—**We review recent studies in which powerful submillimeter radiation has been produced by coherently scattering relatively long wavelength radiation from relativistic electron beams. Various physical mechanisms responsible for the scattering are described and the relationship between them is discussed.**

I. Introduction

In 1968, Pantell *et al.* [1] proposed that strong submillimeter radiation could be produced by coherent scattering of a microwave signal from a counterstreaming relativistic electron beam. The merit of this proposal is clear since it involves the conversion of incident photons at a relatively low frequency ω_0 into an output of scattered photons at a high frequency ω_s via the Doppler effect. According to the Manley–Rowe relationship, the ratio of output wave energy to incident wave energy can be as large as $W_s/W_0 = \omega_s/\omega_0$ and thus good device efficiency is possible.

II. The Doppler Shift

A low-frequency electromagnetic pump wave can be backscattered from an electron stream producing a high-frequency electromagnetic wave if the pump wave vector is antiparallel to the electron velocity. The frequency upshift can be seen by noting that in the reference frame where the electron streaming velocity is zero (i.e., the beam frame in which quantities will be primed) the frequency and wave number of the pump wave are given by

$$\omega_0' = \gamma_\parallel(\omega_0 + \langle v_z\rangle k_0) \tag{1a}$$

$$k_0' = \gamma_\parallel(k_0 + \langle v_z\rangle \omega_0/c^2) \tag{1b}$$

where $\gamma_\parallel = (1 - \langle v_z\rangle^2/c^2)^{-1\,2}$, $\langle v_z\rangle$ is the mean axial velocity of the electron stream in the laboratory frame and (ω_0,k_0) are the frequency and wave number magnitude of the pump wave in the laboratory frame. The direction of the pump wave has been taken to be antiparallel to the direction of the electron stream in the laboratory frame; i.e., $\boldsymbol{k}_0 \cdot \langle \boldsymbol{v}_z\rangle < 0$. Since the scattered wave is backscattered from the electron stream, the wave vector of the scattered wave is parallel to the laboratory frame electron velocity. The frequency of the scattered wave in the laboratory frame then becomes

$$\omega_s = \gamma_\parallel(\omega_s' + \langle v_z\rangle k_s') \tag{2}$$

Manuscript received January 20, 1977.
The authors are with the Naval Research Laboratory, Washington, DC 20375.

where (ω_s',k_s') are the frequency and wave number of the scattered wave in the electron rest frame.

Typically, in the electron rest frame the frequency of the scattered wave is nearly equal to the frequency of the incident pump wave, while the scattered wave vector is opposite in direction but nearly equal in magnitude to the incident wave vector; i.e.,

$$\omega_s' \approx \omega_0' \quad \text{and} \quad k_0' \approx k_s'. \tag{3}$$

Then combining (1)–(3) gives

$$\omega_s \approx \gamma_\parallel{}^2((1 + \langle v_z\rangle^2/c^2)\omega_0 + 2\langle v_z\rangle k_0). \tag{4}$$

If the pump frequency in the laboratory frame is much larger than the characteristic frequencies of the system, the free space dispersion relation $\omega_0 = ck_0$ holds for the pump wave and (4) becomes

$$\omega_s \approx (1 + \langle v_z\rangle/c)^2\gamma_\parallel{}^2\omega_0. \tag{5}$$

It should be appreciated that the frequency conversion factor in (5) $(1 + \langle v_z\rangle/c)^2\gamma_\parallel{}^2$ can be large. For example, if the electron streaming energy is 2 MeV, $\gamma_\parallel = 5$ and $\langle v_z\rangle/c \approx 1$ so that $\omega_s/\omega_0 \approx 100$. Thus a 3-cm pump wave would produce a 300-μm scattered wave.

In the next section, we discuss a physical mechanism that can produce strong electromagnetic scattering from an electron beam and lead to the Doppler-shifted output radiation described above.

III. Stimulated Scattering

Stimulated scattering of photons by an electron ensemble was first predicted by Kapitza and Dirac [2]. In this process, the interaction of the electrons with the electromagnetic pump wave $(\omega_0,\boldsymbol{k}_0)$ and the electromagnetic scattered wave $(\omega_s,\boldsymbol{k}_s)$ is unstable, leading to exponential growth of both the scattered wave and an electron density modulation.

Let us initially consider the details of this process in the beam frame depicted in Fig. 1. The incident pump electromagnetic wave $(\omega_0',\boldsymbol{k}_0')$ has a transverse electric field E_{0y}' which excites a zero-order transverse oscillation of the electrons with velocity

$$v_0' = \hat{e}_y(q/m)E_{0y}'/\gamma'\omega_0' \tag{6}$$

where $\gamma' = [1 - (v_0'/c)^2]^{-1/2}$. In the presence of an incipient backscattered wave $(\omega_s',\boldsymbol{k}_s')$ with magnetic field $B_s'\hat{e}_x$, an axial force $ev_0'B_s'\hat{e}_z$ is exerted on the electrons. The coupling between the scattered electromagnetic wave and

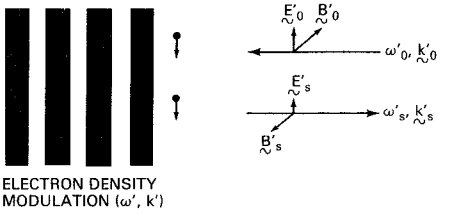

Fig. 1. Stimulated scattering in the beam frame.

the incident wave thus produces a pondermotive force (radiation pressure force) which leads to a low-frequency density modulation of the electrons ($\omega', \boldsymbol{k}'$) and a grouping of the electrons into bunches distributed along the z axis. The complete expression for the pondermotive force is given by $\boldsymbol{F} = -e(\boldsymbol{v}_0' \times \boldsymbol{B}_s' + \boldsymbol{v}_s' \times \boldsymbol{B}_0')$. The frequency and wave number of the electron density modulation satisfies the following conservation laws:

$$\omega' = \omega_0' - \omega_s' \qquad k' = k_0' + k_s' \tag{7}$$

where k', k_0', and k_s' are positive real quantities denoting wave number magnitudes. [It should be noted that typically $\omega' \ll \omega_0'$ and $k' \approx 2k_0'$ so that the approximate equalities of (3) are satisfied.]

The growth of the density modulation gives increasing coherence to the scattering process, resulting in a growing scattered wave which in turn increases the density modulation still further. Thus there is a feedback mechanism in this process which may result in an instability and exponential growth of the scattered wave.

A. Stimulated Raman Scattering and Stimulated Compton Scattering

The growth rate for the stimulated scattering instability depends on a number of factors, viz. the strength of the pump wave, the wavelengths of the incident and scattered waves, the electron density, and the electron temperature. It is useful to distinguish between two regions of parameter space, one in which the Debye length of the electron ensemble is small compared to the electromagnetic wavelengths (stimulated Raman scattering), and the other in which the Debye length to wavelength ratio is not small (stimulated Compton scattering).

The relations between the electron distribution in axial velocity $f(v_z')$ and the phase velocity of the density wave are shown in Fig. 2. For the case of stimulated Raman scattering, as depicted in Fig. 2(a), the magnitude of the density wave phase velocity is much larger than the thermal velocity, i.e.,

$$\frac{\omega'}{k'} \gg v_{\mathrm{TH}}'. \tag{8}$$

In such a situation, the entire electron distribution participates in the density wave which takes the form of a collective plasma oscillation; i.e.,

$$\omega' = \omega_p \tag{9}$$

where ω_p is the invariant plasma frequency. Upon substituting (7) and (9) into (8), one finds that the following

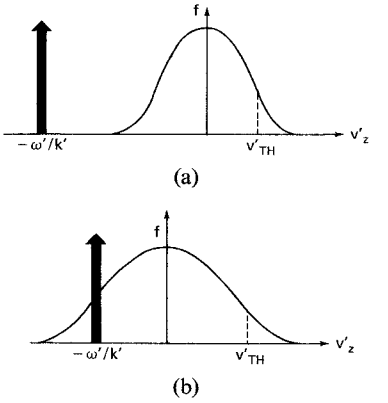

Fig. 2. Relation between the phase velocity of the density disturbance and the electron distribution function. (a) Stimulated Raman scattering. (b) Stimulated Compton scattering.

inequality is implied for the Debye wave number $k_D' = \omega_p/v_{\mathrm{TH}}'$:

$$k_D' \gg k_0' + k_s'. \tag{10}$$

Thus, in the case of stimulated Raman scattering [Fig. 2(a)], the Debye length of the electron ensemble ($\lambda_D' = 2\pi/k_D'$) must be smaller than the wavelength of either the incident or scattered waves.

Stimulated Raman scattering has been analyzed in connection with laser pellet interactions [3] and ionospheric effects [4] as well as the production of submillimeter waves [5], [6]. The expression for the Raman growth rate in an unmagnetized electron stream may be extracted from the literature [5] and takes the form

$$\Gamma_R' \approx (v_0'/c)(\omega_s'\omega_p)^{1/2} \tag{11}$$

where v_0' is given by (6). Equation (11) is the Raman growth rate in the beam frame under the condition that $\omega_p \ll \omega_s'$. The growth rate of (11) depends linearly on the oscillation velocity excited by the pump wave, and in order to have a reasonably large growth rate in a laboratory device, one requires a very strong pump wave source.

In order to satisfy the Raman scattering condition of (10), a dense and cold electron distribution is required. When the electron distribution is tenuous or warm, it becomes difficult to achieve the condition in (10). In that case, the phase velocity of the density disturbance overlays the electron distribution function as shown in Fig. 2(b), and only those electrons in the vicinity of $v_z' \approx \omega'/k'$ participate in the stimulated scattering process. This type of scattering is known as stimulated Compton scattering. Its potential for generating submillimeter waves was first investigated theoretically by Pantel *et al.* [1]. Elaboration was subsequently furnished by Sukhatme and Wolff who considered boundary effects and magnetization [7].

Both Pantell *et al.* and Sukhatme and Wolff used a quantum mechanical formalism. However, the process yields to an equivalent classical analysis. Such an analysis has been carried out [8] and the following expression has been derived for the Compton growth rate:

$$\Gamma_c' \approx (\omega_p^2/\omega_s')|v_0'/v_{\mathrm{TH}}'|^2. \tag{12}$$

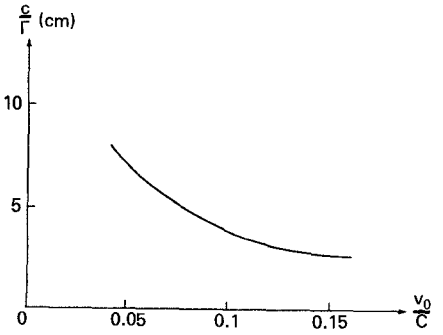

Fig. 3. Exponentiating length for stimulated Raman scattering instability in a magnetized electron beam ($\lambda_0 = 2$ cm, $\lambda_s = 440$ μm, $\gamma = 5$, $\omega_p/2\pi = 3$ GHz, $\Omega/2\pi\gamma = 9$ GHz).

Unlike the Raman growth rate in (11), the Compton growth rate of (12) depends strongly on the electron thermal velocity and decreases rapidly as the electron stream becomes warmer (perhaps as a result of strong scattering).

B. Magnetoresonant Stimulated Raman Scattering

Recently, Sprangle *et al.* [5], [6] have extended the analyses of Raman scattering to produce results which are directly applicable to the production of submillimeter radiation. In this work the growth rate of the backscattered wave was shown to increase when an external constant magnetic field $B_0\hat{e}_z$ was applied and its strength adjusted so that $\omega_0' \approx \Omega_0$, where $\Omega_0 = |e|B_0/m_0c$ is the electron cyclotron frequency. The transverse electron velocity in the beam frame then becomes

$$v_0' = \frac{|e|}{\gamma' m_0} E_{0y}' \frac{\omega_0'}{\omega_0' - \Omega_0} \hat{e}_y. \tag{13}$$

In (13), the pump frequency ω_0' must satisfy a dispersion relation. The dispersion relation of the pump wave in the magnetized electron stream in the beam frame is

$$\omega_0'^2 - c^2 k_0'^2 - \omega_p^2 \omega_0'/(\omega_0' - \Omega_0) = 0. \tag{14}$$

Hence $\omega_0' - \Omega_0$ cannot be made arbitrarily small and is determined by the dispersion relation in (14).

The temporal growth rate for the stimulated magnetoresonant scattering process has been derived in the beam frame as [5]

$$\Gamma_M' \approx \frac{v_0'}{c} \omega_s' \left(\frac{\omega_p'}{\omega_s' + \Omega_0/2} \right)^{1/2}. \tag{15}$$

The laboratory frame growth rate for the stimulated scattering instability may be found from the beam frame growth rate through the relationship [8] $\Gamma = \gamma_\parallel^{-1}(1 + v_g'\langle v_z\rangle/c^2)^{-1}\Gamma'$ where v_g' is the group velocity of the pump wave in the beam frame. Thus one could calculate growth rates in the beam frame and then transform to the laboratory frame. On the other hand, fully relativistic calculations have been carried out directly in the laboratory frame. Results for parameters characteristic of an intense relativistic electron beam (2 MV, 30 kA) are presented in Fig. 3 as a plot of c/Γ versus v_0/c. It will be noted that when the oscillation velocity induced by the pump wave is one-tenth the speed of light ($v_0/c = 0.1$), the e-folding length for the instability is on the order of a few centimeters, short enough to be of practical interest. The pump wave field required to achieve the condition $v_0/c = 0.1$ is of order $E_0 \sim 10^5$ V/cm, corresponding to a power density in the pump wave of tens of megawatts per square centimeter.

Frequency relationships which hold for magnetoresonant stimulated Raman scattering are depicted in the (ω,k) diagrams of Fig. 4. Both beam frame and laboratory frame relationships are shown for the case of a modest ω_s/ω_0 ratio, and both the incident electromagnetic wave and the scattered wave are assumed to be RHCP. The parallelograms with one side represented by the density wave, with a second side represented by the scattered wave, and with the diagonal represented by the pump wave are called Stokes diagrams. It may be clearly seen that in the beam frame ω_s' is slightly smaller than ω_0'. However, upon transformation to the laboratory frame, ω_s becomes considerably larger than ω_0 while the Stokes diagram relationship between the three waves is still maintained.

C. Saturation of the Stimulated Scattering Process

A number of mechanisms may be responsible for saturating the backscattered wave. For example, in the case of stimulated Raman scattering, thermalization of the electron stream to the point where $v_{TH}' \approx \omega'/k'$ will result in the trapping of the electrons in the potential well of the density wave, thus stopping the scattering process.

In the stimulated Compton regime, saturation occurs when the electrons fall to the bottom of the potential well associated with the density fluctuation. Therefore, for an instability to occur in the Compton region, the Compton growth rate must be much greater than the frequency of oscillation (bounce frequency) of the electrons in the potential well. Since the bounce frequency is proportional to the square root of the amplitude of the longitudinal fluctuation, an estimate for the maximum amplitude can be obtained.

Finally, depletion of the energy in the pump wave may also place limits on the energy in the backscattered wave. Work on evaluating the various saturation mechanisms is only just beginning, and estimates of device efficiency in terms of electron beam energy are as yet unavailable.

IV. Laboratory Demonstrations of Submillimeter-Wave Production by Stimulated Scattering

As described in Section III-B, the observation of stimulated scattering in a laboratory device requires exceptionally large pump wave power. This has led to some novel experimental arrangements for pump wave production. First, an intense relativistic electron beam has been used to generate the pump wave as well as to provide the medium in which the stimulated scattering occurs. Secondly, a long, spatially periodic, magnetic field has been used as a quasi-pump wave. Each of these approaches will be discussed in turn.

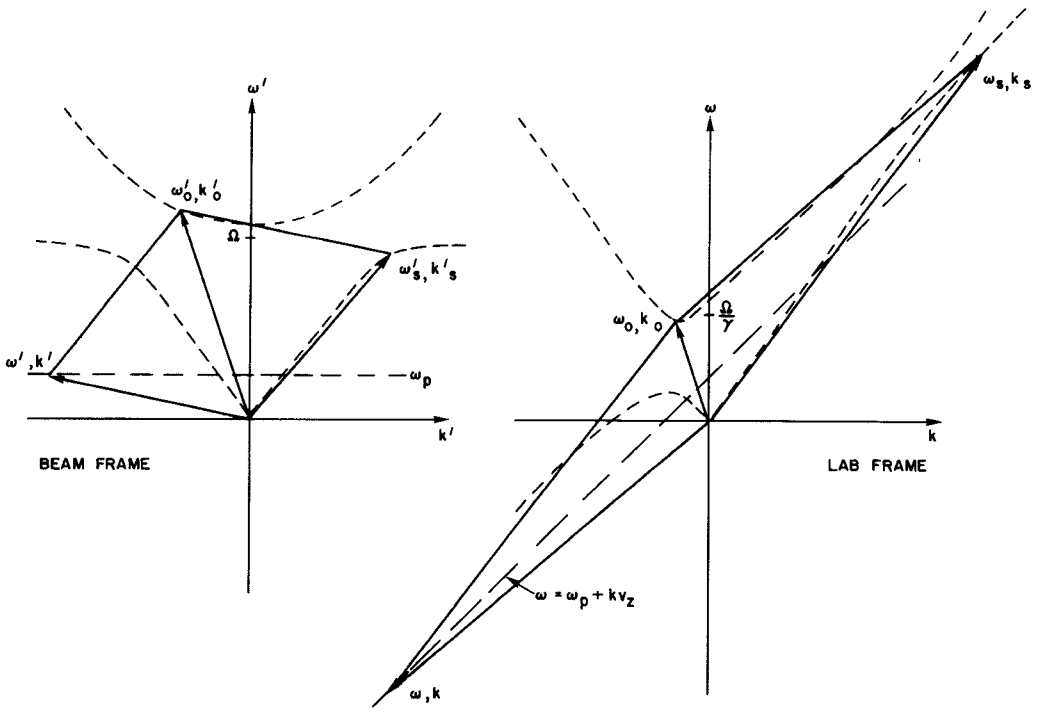

Fig. 4. Stokes diagrams for stimulated Raman scattering from a magnetized electron beam. ----- Dispersion curves for RHCP waves. — — — Dispersion curves for space charge waves.

A. Generating a Pump Wave with an Intense Relativistic Electron Beam

At the First International Conference on Submillimeter Waves and Their Applications (Atlanta, GA, 1974), the production of strong submillimeter radiation was reported [9] in an experiment that had been originally designed for generating 2-cm microwaves with an intense relativistic electron beam. Subsequent calculations [6] showed that a quantitatively consistent explanation for the submillimeter radiation could be obtained from a model in which a fraction of the 2-cm radiation was spuriously reflected off the microwave output window, and subsequently took part in a stimulated scattering process with a cold streaming part of the intense e beam. The submillimeter radiation was only observed when the electron accelerating voltage $\gtrsim 1.5$ MV; one may easily confirm that this roughly corresponds to the electron energy necessary to produce a Doppler shift from a 2-cm incident wave to a 0.5-mm backscattered output wave.

Recently, further studies have been described in which the initial experimental configuration was modified to strengthen the process described above [10]. The modified experimental configuration is shown schematically in Fig. 5. The e beam was passed through a nonadiabatic perturbation in the applied magnetic field which converted a large fraction of the electron streaming energy into energy transverse to the axis of the drift tube (inner diameter = 4.7 cm). The electrons with large transverse energy then reacted unstably with an electromagnetic mode of the drift tube (cyclotron maser process [11]) and produced a 2-cm

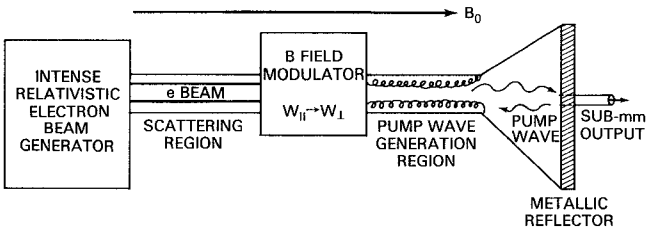

Fig. 5. Experimental configuration in which magnetoresonant stimulated Raman scattering has been demonstrated. (One intense relativistic e beam is used both to generate the pump wave and to effect stimulated scattering.)

pump wave having a power of hundreds of megawatts. This pump wave was reflected off a metallic plate, and traveled back up the drift tube toward the cathode. When the pump wave encountered the cold streaming electrons near the cathode, stimulated Raman scattering occurred resulting in backscattered submillimeter waves.

The submillimeter output power has been optimized by varying both the uniform magnetic field level and the position of the magnetic modulator. As a confirmation of the importance of the cold streaming electrons in the scattering region, it was found that the submillimeter output increased as the scattering region was made longer, while, on the other hand, it became weaker when the electrons in the scattering region had some of their streaming energy prematurely converted to transverse energy. For parameters close to those cited in the caption of Fig. 3, an output power of ~ 1 MW was measured at $\lambda \sim 400$ μm, and the submillimeter generation process was judged to be magnetoresonant stimulated Raman scattering.

The experimental configuration depicted in Fig. 4 has a

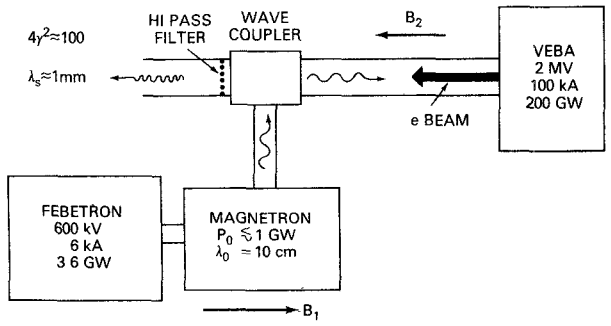

Fig. 6. Planned experimental configuration for demonstrating optimized magnetoresonant Raman scattering. (Two intense relativistic e-beam generators are used. One to generate the pump wave, and the second to effect stimulated scattering.)

distinct disadvantage in that both pump wave generation and stimulated scattering occur in the same e beam. This does not allow for separate optimization of each process and complicates interpretation of the experimental results. Furthermore, the pump wave may be significantly attenuated as it travels back through the perturbed electrons in the pump wave generation region before entering the scattering region. To overcome these disadvantages, the new experimental configuration pictured in Fig. 6 is presently being assembled at the Naval Research Laboratory. Two separate electron accelerators are being employed. The smaller Febetron accelerator (beam power $\approx$ 4 GW) will be used to drive a relativistic magnetron [12] that will furnish a $\lambda_0 = 10$-cm, $P_0 = 1$-GW pump wave. The VEBA accelerator [13] (beam power $\approx$ 200 GW) will provide the electron beam in which magnetoresonant stimulated Raman scattering may take place. The backscattered output radiation is expected to be at $\lambda_s \approx 1$ mm. Potentially, a large fraction of the VEBA e-beam energy may appear in this scattered wave. (Note that $P_0\omega_s/\omega_0 \sim$ 100 GW.)

B. A Spatially Periodic Magnetic Field as a Pump Wave

Instead of using an ultrapowerful, fast, electromagnetic wave as a laboratory pump wave, one may instead pass the relativistic electron beam through a magnetic field which is periodically rippled along the flow axis. Such a rippled field may be regarded as a quasi-wave, and is represented in simplified form by the parameters $\boldsymbol{E}_0 = 0$, $\boldsymbol{B}_0 = b_r\hat{e}_x$, $\omega_0 = 0$, and $k_0 = 2\pi/L$ where L is the ripple period. In the beam frame, the quasi-wave will have an electric field

$$E_{0y}' = \gamma_\parallel(E_{0y} + \langle v_z\rangle \boldsymbol{B}_{0x}) = \gamma_\parallel\langle v_z\rangle b_r \qquad (16)$$

and a frequency

$$\omega_0' = \gamma_\parallel(\omega_0 + k_0\langle v_z\rangle) = \gamma_\parallel \frac{2\pi}{L}\langle v_z\rangle. \qquad (17)$$

It is easily verified from (16) that if $\langle v_z\rangle$ is relativistic, then a modest value of b_r on the order of kilogauss is equivalent to a very powerful electromagnetic pump wave.

Then, all the considerations discussed in the previous sections for the occurrence of stimulated scattering apply. From (2)

$$\omega_s \approx \omega_s'/\gamma_\parallel(1 - \langle v_z\rangle/c) = (1 + \langle v_z\rangle/c)\gamma_\parallel\omega_s'$$

and then using (3) and (17), one has

$$\lambda_s = L/[(1 + \langle v_z\rangle/c)(\langle v_z\rangle/c)\gamma_\parallel{}^2].$$

Thus the scattered wavelength is reduced from the length of the ripple period by the large Doppler shift factor.

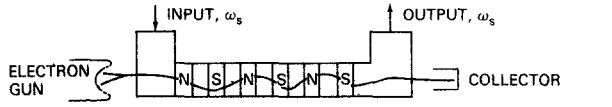

Fig. 7. Configuration for stimulated scattering experiments in which spatially periodic magnetic field acts as pump wave.

We believe an experiment carried out by Elias *et al.* at Stanford University [14] may be interpreted as stimulated Compton scattering using a rippled magnetic field as a pump wave. Their experimental arrangement is shown schematically in Fig. 7. A 70-mA beam of 24-MeV electrons was passed through a helical 2.4-kG magnetic field of period 3.2 cm and length 5.2 m. A 10.6-μm signal was amplified in this system with a gain of 7 percent per pass. The gain was found to be independent of the power density at 10.6 μm over a range of 100–1.4 $\times$ 10^5 W/cm^2.

A related experiment employing a rippled magnetic field pump wave has been carried out by Mross *et al.* [15] at Columbia University. In their experiment the electron energy was $\sim$800 keV and the output wavelength was $\lambda_s \approx 1$ mm, while the electron density was large enough to allow for collective plasma oscillations (stimulated Raman scattering). Analytical [8], [16] and numerical [17] studies of the interaction of a relativistic electron beam with a rippled magnetic field have also been carried out.

V. Other Coherent Scattering Mechanisms

The processes discussed above by no means exhaust the possible coherent scattering mechanisms that can yield submillimeter radiation by upconversion of a relatively long wavelength incident wave. Schneider and Spitzer [18] have suggested the exploitation of a synergistic effect combining stimulated Compton scattering with the shock wave effect produced when an electron beam travels faster than the speed of light in a background gas.

The scattering of an incident electromagnetic wave by the moving refractive-index discontinuity represented by the front of an intense relativistic electron beam has been reported by Granatstein *et al.* [19]; in a preliminary experiment, a 3-cm incident wave at 150 kW was scattered to produce an 8-mm output wave at 300 kW. A similar frequency shift has also been observed in beam front scattering experiments carried out by Buzzi *et al.* [20]. Lampe *et al.* [21] have suggested that a propagating ionization front could be used in place of the electron beam front.

It is evident that a growing number of research workers are intrigued by processes which produce submillimeter

radiation through coherent scattering and Doppler frequency upshift. The very attractive potential for having simultaneously both power gain and frequency conversion is likely to draw forth still other suggestions for coherent scattering mechanisms in the future.

Acknowledgment

The authors wish to thank their colleagues at the Naval Research Laboratory who have greatly added to their understanding of coherent scattering processes, in particular, W. M. Manheimer and A. Drobot.

References

[1] R. H. Pantell, G. Soncini, and H. E. Puthoff, "Stimulated photon-electron scattering," *IEEE J. Quantum Electron.*, vol. QE-4, pp. 905–907, 1968.

[2] P. L. Kapitza and P. A. M. Dirac, "The reflection of electrons from standing light waves," *Proc. Cambridge Phil. Soc.*, vol. 29, pp. 297–300, 1933.

[3] W. M. Manheimer and E. Ott, "Parametric instabilities induced by the coupling of high and low frequency plasma modes," *Phys. Fluids*, vol. 17, pp. 1414–1421, 1974.

[4] F. W. Perkins and P. K. Kaw, "On the role of plasma instabilities in ionospheric heating by radio waves," *J. Geophys. Res.*, vol. 76, pp. 282–284, 1971.

[5] P. Sprangle and V. L. Granatstein, "Stimulated cyclotron resonance scattering and production of powerful submillimeter radiation," *Appl. Phys. Lett.*, vol. 25, pp. 377–379, 1974.

[6] P. Sprangle, V. L. Granatstein, and L. Baker, "Stimulated collective scattering from a magnetized relativistic electron beam," *Phys. Rev. A*, vol. 12, pp. 1697–1701, 1975.

[7] V. P. Sukhatme and P. E. Wolff, "Stimulated compton scattering as a radiation source-theoretical limitation," *J. Appl. Phys.*, vol. 44, pp. 2331–2334, 1973; "Stimulated magneto-Compton scattering—A possible tunable far infrared and millimeter wave source," *IEEE J. Quantum Electron.*, vol. QE-10, pp. 870–873, 1974.

[8] A. Hasegawa, K. Mina, P. Sprangle, H. H. Szu, and V. L. Granatstein, "Limitation in growth time of stimulated Compton scattering in X-ray regime," *Appl. Phys. Lett.*, vol. 29, pp. 542–544, 1976.

[9] V. L. Granatstein, M. Herndon, R. K. Parker, and S. P. Schlesinger, "Strong submillimeter radiation from intense relativistic electron beams," *IEEE Trans. Microwave Theory Tech.*, vol. MTT-22, pp. 1000–1005, 1974.

[10] V. L. Granatstein, S. P. Schlesinger, M. Herndon, R. K. Parker, and J. A. Pasour, "Production of megawatt submillimeter pulses by stimulated magneto-Raman scattering," *Appl. Phys. Lett.*, to be published.

[11] J. L. Hirshfield and J. M. Wachtell, "Electron cyclotron maser," *Phys. Rev. Lett.*, vol. 12, pp. 533–536, 1964.

[12] G. Bekefi and T. J. Orzechowski, "Giant microwave bursts emitted from a field-emission, relativistic-electron-beam magnetron," *Phys. Rev. Lett.*, vol. 37, pp. 379–382, 1976.

[13] R. K. Parker and M. Ury, "The VEBA relativistic electron accelerator," *IEEE Trans. Nuclear Sci.*, vol. NS-22, pp. 983–988, 1975.

[14] L. Elias, W. Fairbank, J. M. J. Madey, H. A. Schwettman, and T. Smith, "Observation of stimulated emission of radiation by relativistic electrons in a spatially periodic transverse magnetic field," *Phys. Rev. Lett.*, vol. 36, pp. 717–720, 1976.

[15] M. R. Mross, T. C. Marshall, P. Efthimion, and S. P. Schlesinger, "Submillimeter wave generation through stimulated scattering with an intense relativistic electron beam and zero frequency pump," *Digest Second Int. Conf. Winter School on Submillimeter Waves and Their Applications* (IEEE Cat. No. 76 CH 1152-8 MTT), pp. 128–129, 1976.

[16] F. A. Hopf, P. Meystre, M. O. Scully, and W. H. Louisell, "Strong signal theory of a free electron laser," *Phys. Rev. Lett.*, vol. 37, pp. 1342–1345, 1976.

[17] T. Kwan, J. M. Dawson, and A. T. Lin, "The free electron laser," Report No. PPG-267, Rept. of Physics, UCLA, 1976.

[18] S. Schneider and R. Spitzer, "Application of stimulated electromagnetic shock radiation to the generation of intense submillimeter waves," this issue, pp. 551–555.

[19] V. L. Granatstein, P. Sprangle, R. K. Parker, J. Pasour, M. Herndon, and S. P. Schlesinger, "Realization of a relativistic mirror: Electromagnetic backscattering from the front of a magnetized relativistic electron beam," *Phys. Rev. A*, vol. 14, pp. 1194–1201, 1976.

[20] J. M. Buzzi *et al.*, "Experimental evidence of relativistic Doppler frequency conversion on a relativistic electron beam front," this issue, pp. 559–560.

[21] M. Lampe, E. Ott, W. M. Manheimer, and S. Kainer, "Submillimeter-wave production by upshifted reflection from a moving ionization front," this issue, pp. 556–558.